Journal of Hazardous Materials 164 (2009) 329–336

Contents lists available at ScienceDirect

Journal of Hazardous Materials

journal homepage: www.elsevier.com/locate/jhazmat

Molecular dynamics study of binding energies, mechanical properties, and detonation performances of bicyclo-HMX-based PBXs

Ling Qiu[a,b], Heming Xiao[a,*]

[a] Institute for Computation in Molecular and Material Science, School of Chemical Engineering, Nanjing University of Science and Technology, Nanjing 210094, PR China
[b] Key Laboratory of Nuclear Medicine, Ministry of Health, Jiangsu Institute of Nuclear Medicine, Wuxi 214063, PR China

ARTICLE INFO

Article history:
Received 7 April 2008
Received in revised form 4 August 2008
Accepted 6 August 2008
Available online 19 August 2008

Keywords:
Molecular dynamics (MD)
Polymer-bonded explosive (PBX)
Binding energies
Mechanical property
Detonation performance

ABSTRACT

To investigate the effect of polymer binders on the monoexplosive, molecular dynamics simulations were performed to study the binding energies, mechanical properties, and detonation performances of the bicyclo-HMX-based polymer-bonded explosives (PBXs). The results show that the binding energies on different crystalline surfaces of bicyclo-HMX decrease in the order of (0 1 0) > (1 0 0) > (0 0 1). On each crystalline surface, binding properties of different polymers with the same chain segment are different from each other, while those of the polymers in the same content decrease in the sequence of PVDF > F_{2311} > F_{2314} ≈ PCTFE. The mechanical properties of a dozen of model systems (elastic coefficients, various moduli, Cauchy pressure, and Poisson's ratio) have been obtained. It is found that mechanical properties are effectively improved by adding small amounts of fluorine polymers, and the overall effect of fluorine polymers on three crystalline surfaces of bicyclo-HMX changes in the order of (0 1 0) > (0 0 1) ≈ (1 0 0). In comparison with the base explosive, detonation performances of the PBXs decrease slightly, but they are still superior to TNT. These suggestions may be useful for the formulation design of bicyclo-HMX-based PBXs.

1. Introduction

cis-1,3,4,6-Tetranitrooctahydroimidazo-[4,5-d]imidazole, commonly called 'bicyclo-HMX' because of its structural analogy with HMX (1,3,5,7-tetranitro-1,3,5,7-tetrazocane), is an important explosive and can be employed in solid pyrotechnic compositions, for example in solid propellants or in plastic-bonded explosives. Fig. 1 shows a schematic illustration of the molecular and crystal structures of bicyclo-HMX, and the numbering of the atoms that will be used in subsequent discussions is also shown. As can be seen, it contains fewer H atoms and larger ring strain than HMX and may be able to exhibit superior explosive performance to HMX, which is one of the most powerful widely used explosives. Therefore, it inspired a significant history of interest in the structural and explosive properties since it was first reported [1–14].

As well known, explosives used in practice are usually the mixtures not the compounds, such as the typical polymer-bonded explosives (PBXs), which are highly filled composite materials comprising grains of an explosive held together by small amounts of one or more kinds of polymer binders. They have been widely used in both civilian and military fields for a long time because they have notable merits such as good safety, high strength, easiness of process, and so on [15–18]. The polymer binder in the PBX plays an important role in improving the properties of the base explosive, such as improving mechanical properties, decreasing signature, extending service life, reducing environmental impact, etc. Therefore, researches on the composite material PBXs have been becoming a hot topic. Heretofore, a lot of effort has been put into studying the explosives and polymers with experimental measurements [19–23], calculations or simulations by quantum mechanics (QM), molecular mechanics (MM), and molecular dynamics (MD) [24–26]. Recently, a series of MD simulations have also been performed by us to study the structures and properties of TATB (2,4,6-trinitrobenzene-1,3,5-triamine), HMX, TNAD (*trans*-1,4,5,8-tetranitrodecahydropyrazino[2,3-b]pyrazine), and CL-20 (2,4,6,8,10,12-hexanitro-2,4,6,8,10,12-hexaazaisowurtzitane)-based PBXs [27]. The effect of polymer binders in improving the mechanical properties of explosives was particularly studied. However, as far as we know, no report has been found on the investigation of the bicyclo-HMX-based PBXs. Hence, for understanding profoundly the performances of the base explosive and guiding the formulation design of PBXs, a detailed research on the polymer effect on the structure and properties of bicyclo-HMX is necessary.

In this paper, four typical fluorine polymers, PVDF (polyvinylidenedifluoride), PCTFE (polychlorotrifluoroethylene), F_{2311} and F_{2314}, were chosen to construct the binary PBXs by blending the

* Corresponding author. Tel.: +86 25 84303919; fax: +86 25 84303919.
E-mail address: xiao@mail.njust.edu.cn (H. Xiao).

0304-3894/$ – see front matter.
doi:10.1016/j.jhazmat.2008.08.030

base explosive bicyclo-HMX with polymers on three crystalline surfaces (0 0 1), (0 1 0), and (1 0 0), respectively. F_{2311} and F_{2314} are copolymerized from vinylidenedifluoride and chlorotrifluoroethylene with the molar ratios of 1:1 and 1:4, respectively. Classical MD simulations were performed on both the PBXs and the pure crystal for comparison. The interactions between the polymers and bicyclo-HMX were analyzed by calculating the binding energies. Mechanical properties and detonation performances were predicted for the PBXs and the pure explosive by the elastic-static method and theoretical method, respectively. Differences in the binding energies, mechanical properties, and detonation performances among different PBXs were examined. The correlations among the type and content of the polymers, binding energies, mechanical properties, and detonation performances are established, which are expected to be useful for the formulation design of novel PBXs.

2. Computational method

2.1. Computational model

The crystal structure of bicyclo-HMX used in the condensed phase simulations was taken from Gilardi et al. [10], which crystallized in the monoclinic space group of $P2_1$ with five independent lattice parameters $a = 8.598$ Å, $b = 6.950$ Å, $c = 8.973$ Å, $\alpha = \gamma = 90^\circ$, and $\beta = 101.783^\circ$. There are two irreducible molecules in the unit cell, see Fig. 1. Four kinds of fluorine polymers were built and processed by the Amorphous Cell module as implemented in the commercial software Accelrys Materials Studio (MS) 3.0.1 [28]. Each polymer chain consists of 10 chain segments, and the end groups are saturated by the H or F atoms according to their types. Afterwards, 2.5 ns MD simulations were carried out to get the equilibrium conformations of polymers.

Taking into account the computation resource, a periodic MD simulation cell consisting of 72 molecules was selected for bicyclo-HMX to make the simulation model approach the practice sufficiently, which was obtained by replicating the unit cell fourfold for the a crystallographic axis and threefold for the b and c crystallographic axes, respectively, i.e. a $4 \times 3 \times 3$ box of unit cells. Then, to investigate the differences among the properties of various crystalline surfaces, taking an example, the supercell was cleaved along three crystalline surfaces (1 0 0), (0 1 0), and (0 0 1), respectively. Then, the periodic supercells were further separated from the repeated replicas by a vacuum layer of 10 Å along the c crystallographic axis, respectively. According to the practical formulation of the commonly used PBXs, such as HMX and RDX-based PBXs, where the content of the polymer binders is 5–10 wt.%, we should adopt an appropriate quantity of polymers to be placed in each supercell. In the present study, we embed two equilibrium chains of each kind of polymer into the supercell model in parallel with different crystalline surfaces. A total of 12 PBX models with 1996 atoms were constructed.

2.2. Simulation detail

Minimizations are initially carried out for 5000 iterations to equilibrate the PBXs models and then the simulation boxes are compressed slightly (0.3%) along the c direction. Afterward, another 5000 iterations of minimizations are carried out to reach the equilibrium state and the boxes are compressed further along the c direction. The above processes are repeated step by step (the configuration in each step should be minimized to reach the equilibrium) until the density approaches the theoretical maximum value, which can be predicted according to the weight percent of each component in the PBXs.

Starting from the above-minimized structures, MD simulations are subsequently carried out in the NVT (constant number of particles, volume, and temperature) ensemble with the general force field COMPASS (condensed-phase optimized molecular potentials for atomistic simulation studies) [29]. The systems are first integrated for 1×10^5 time steps in all equilibration runs, which are necessary to reach the mechanical and thermal equilibrium; then followed by the production runs of 2×10^5 time steps, during which data are collected for subsequent analysis. A fixed time step size of 1 fs is used in all cases. The coordinate trajectory of the system is collected every 1000 time steps and a total of 200 trajectory files are obtained. The Andersen thermostat method [30] is employed to control the system at the temperature of 298 K. In all of the simulations, usual periodic boundary conditions have been applied to motion parallel to the surface and no-periodic ones for motion perpendicular to the surface. The surface is modeled as a true boundary, including the atoms in the surface. The opposite side of the box is also treated as a boundary; when a molecule strays out the top side of the box, it is reflected back into the simulation cell. The equations of motion for the molecules and simulation cells are integrated using the Verlet leapfrog scheme [31]. The interactions are determined between the sites in the simulation box and the nearest-image sites within the cutoff distance of 9.5 Å. The Coulomb and van der Waals long-range, nonbond interactions are handled by using the standard Ewald and Atom-Based summation methods, respectively [31]. The electrostatic charges are determined and assigned automatically by the selected COMPASS force field. The elastic tensors and mechanical properties were esti-

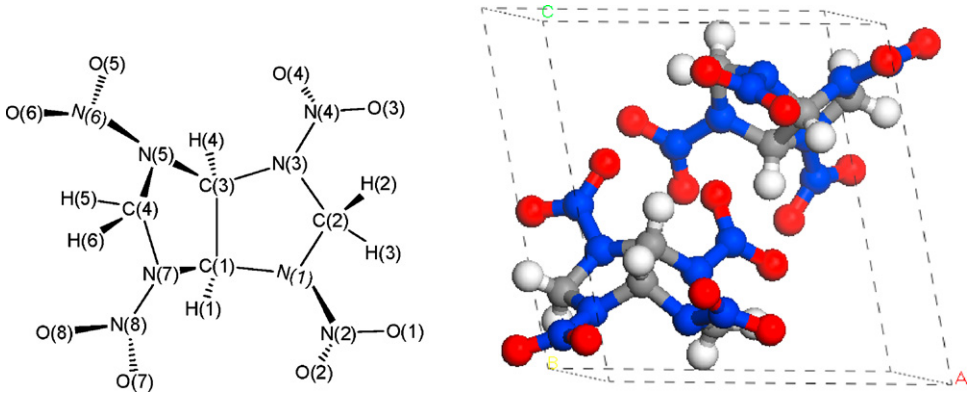

Fig. 1. Schematic view of the conformations for bicyclo-HMX molecule and crystal. Gray, blue, red, and white spheres stand for C, N, O, and H atoms, respectively. (For interpretation of the references to colour in this figure legend, the reader is referred to the web version of the article.)

Table 1
Comparison of the simulated lattice parameters and atomic coordinates based on the COMPASS force field with the experimental values for bicyclo-HMX[a]

Method	Lattice parameters							
	a (Å)	b (Å)	c (Å)	α (°)	β (°)	γ (°)	V (Å^3)	ρ (g cm^{-3})
Exp.[10]	8.598	6.950	8.973	90.0	101.783	90.0	524.826	1.861
NVT-MD	8.598(0.0)	6.950(0.0)	8.973(0.0)	90.0(0.0)	101.783(0.0)	90.0(0.0)	524.826(0.0)	1.861(0.0)
NPT-MD	7.953(7.50)	7.351(5.77)	8.758(−2.40)	90.0(0.0)	101.274(−0.50)	90.0(0.0)	517.039(−1.48)	1.891(1.61)
MM	7.909(−8.01)	7.355(5.83)	8.849(−1.38)	90.0(0.0)	103.516(1.70)	90.0(0.0)	500.458(−4.64)	1.952(4.89)

Atom	Atomic coordinates											
	Exp.[10]			NVT-MD			NPT-MD			MM		
	x	y	z	x	y	z	x	y	z	x	y	z
C1	0.1760	0.1529	0.2716	0.2026	0.1486	0.2916	0.2071	0.1525	0.2843	0.2081	0.1537	0.2830
C2	−0.0147	0.4210	0.2334	−0.0196	0.4095	0.2570	−0.0184	0.4046	0.2637	−0.0182	0.4062	0.2637
C3	0.2508	0.3261	0.3678	0.2866	0.3263	0.3628	0.3054	0.3203	0.3548	0.3119	0.3195	0.3542
C4	0.3858	0.2678	0.1574	0.3730	0.2470	0.1358	0.3848	0.2303	0.1197	0.3840	0.2333	0.1185
N1	0.0277	0.2328	0.1859	0.0494	0.2188	0.2075	0.0448	0.2266	0.1995	0.0449	0.2331	0.1961
N2	−0.0923	0.1093	0.1244	−0.0623	0.1038	0.1212	−0.0799	0.1237	0.1065	−0.0825	0.1327	0.0971
N3	0.1255	0.4685	0.3480	0.1604	0.4669	0.3647	0.1751	0.4553	0.3670	0.1793	0.4525	0.3714
N4	0.1029	0.5762	0.4688	0.1659	0.6173	0.4645	0.1930	0.5916	0.4774	0.1985	0.5931	0.4782
N5	0.3803	0.3785	0.2938	0.3912	0.3793	0.2603	0.4018	0.3684	0.2363	0.4035	0.3750	0.2345
N6	0.5115	0.4669	0.3746	0.5371	0.4707	0.3079	0.5498	0.4752	0.2683	0.5525	0.4810	0.2689
N7	0.2824	0.1037	0.1698	0.2971	0.0801	0.1836	0.3087	0.0747	0.1814	0.3050	0.0785	0.1757
N8	0.3583	−0.0773	0.1965	0.3720	−0.0971	0.2012	0.3947	−0.0867	0.2200	0.3959	−0.0832	0.2136
O1	−0.2217	0.1836	0.0775	−0.1872	0.1728	0.0674	−0.2124	0.2009	0.0523	−0.2168	0.2100	0.0393
O2	−0.0570	−0.0609	0.1172	−0.0262	−0.0645	0.1122	−0.0454	−0.0343	0.0861	−0.0489	−0.0248	0.0767
O3	−0.0202	0.6709	0.4475	0.0478	0.7122	0.4529	0.0673	0.6870	0.4783	0.0705	0.6847	0.4757
O4	0.2032	0.5730	0.5844	0.2859	0.6398	0.5588	0.3271	0.5977	0.5678	0.3387	0.6103	0.5681
O5	0.5030	0.5300	0.4998	0.5671	0.5272	0.4376	0.5879	0.5336	0.3997	0.5947	0.5431	0.3989
O6	0.6228	0.4830	0.3108	0.6271	0.4747	0.2206	0.6274	0.4929	0.1636	0.6319	0.4993	0.1683
O7	0.2907	−0.2001	0.2538	0.3159	−0.2152	0.2745	0.3349	−0.1854	0.3056	0.3379	−0.1886	0.2938
O8	0.4802	−0.0977	0.1505	0.4863	−0.1184	0.1483	0.5193	−0.1158	0.1658	0.5258	−0.1062	0.1658
H1	0.1579	0.0436	0.3351	0.1816	0.0368	0.3709	0.1813	0.0570	0.3734	0.1835	0.0524	0.3669
H2	−0.1092	0.4161	0.2766	−0.0828	0.4199	0.3120	−0.0856	0.4064	0.3271	−0.0885	0.3992	0.3243
H3	−0.0310	0.5121	0.1497	−0.0068	0.5127	0.1621	−0.0099	0.5071	0.1700	−0.0194	0.5110	0.1731
H4	0.2887	0.2919	0.4751	0.3552	0.3024	0.4800	0.3934	0.3017	0.4658	0.4047	0.2975	0.4659
H5	0.4932	0.2260	0.1564	0.4874	0.2104	0.1054	0.5100	0.1945	0.0890	0.5092	0.1964	0.0930
H6	0.3456	0.3421	0.0662	0.2967	0.3025	0.0308	0.3038	0.2758	0.0132	0.3008	0.2806	0.0073

[a] NVT-MD and NPT-MD denote the molecular dynamics simulations performed within NVT and NPT ensembles at 298 K based on the COMPASS force field, respectively; MM denotes the molecular mechanics calculation with the COMPASS force field at 0 K. Andersen thermostat method and Parrinello barostat method have been employed in the NPT-MD simulations to control the system at 298 K and ambient pressure, respectively. The values in parentheses are the percentage difference relative to the experimental data.

mated by the static mechanics method as implemented in the MS 3.0.1 program. All calculations were performed on a Pentium-IV PC.

3. Results and discussion

3.1. Choice of force field and equilibrium of system

The COMPASS force field is chosen in present MD simulations as in our previous studies [27]. On the one hand, its parameters have been debugged and ascertained from ab initio calculations, optimized according to the experimental values, and parameterized using extensive data for molecules in the condensed phase. Its nonbond parameters have been further amended and validated by thermal physical properties of molecules in the liquid and solid phases. Consequently, COMPASS is able to make accurate predictions of structural, conformational, vibrational, and thermophysical properties for a broad range of compounds both in isolated and condensed phases. Extensive validations have been performed [32–34]. On the other hand, this force field has been successfully employed to investigate the typical nitramine explosives HMX, TNAD, CL-20, and their PBXs [27a–c]. It is therefore expected to be also suitable for studying bicyclo-HMX. This has been verified by comparing the simulated crystal structure with the experimental data in Table 1. As can be seen, the predicted lattice parameters and atomic coordinates are in reasonable agreement with those from experiment. On account of bicyclo-HMX being the main body of the PBXs, hence in subsequent studies the COMPASS force field is used in MD simulations of the bicyclo-HMX-based PBXs.

With respect to the static mechanical analysis, the system must reach the equilibrium state. There are two criteria to judge the equilibrium of system: one is the equilibrium of temperature and the other is the equilibrium of energy. When the fluctuations of temperature and energy are in the range of 5–10%, the equilibrium of system is ascertained. Generally, the system achieves equilibrium in first 50 ps; an additional 50 ps are allowed to ensure the equilibrium in every case. For example, Fig. 2 shows the fluctuation curves of temperature and energy in the equilibration run of the PBX with F_{2314} on the (0 1 0) crystalline surface. One observes that the system quickly equilibrates in less than 50 ps and then continues to fluctuate around the equilibrium state. The temperature fluctuates within ±15 K when it reaches the equilibrium state. The deviations of potential energy and nonbond energy are less than 0.7% and 0.4%, respectively, indicating that the system has reached its energy equilibrium. Similarly, other PBXs all come to the equilibrium according to these two criteria. As an illustration, the equilibrium configurations of the PBXs with F_{2314} on bicyclo-HMX crystalline surfaces (0 0 1), (0 1 0), and (1 0 0) are presented in Fig. 3.

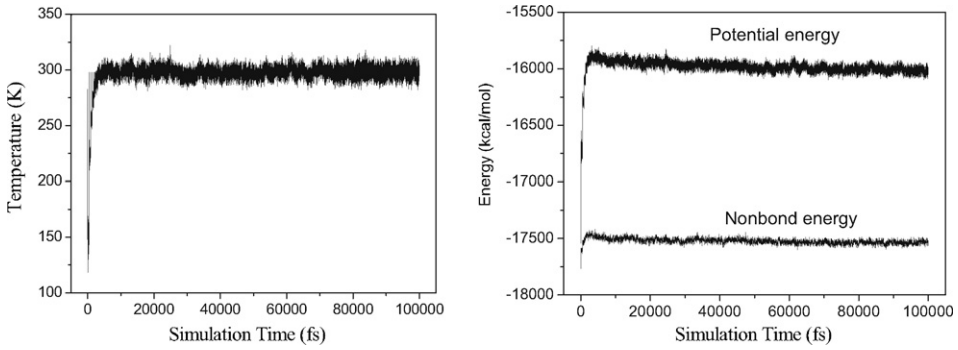

Fig. 2. Fluctuation curves of temperature and energy in the MD equilibration run for the PBX with F_{2314} on bicyclo-HMX (0 1 0) crystalline surface at the temperature of 298 K.

3.2. Binding energy

Binding energy ($E_{binding}$) can well reflect the intermolecular interactions between the polymers and the base explosive, which is defined as the negative value of the interaction energy (E_{inter}). It also well reflects the capacity of polymer binders to blend with the explosive. E_{inter} can be evaluated by the total energy of the PBX and its corresponding components in the equilibrium state. So, $E_{binding}$ between bicyclo-HMX and fluorine polymers can be figured out by the following expression:

$$E_{binding} = -E_{inter} = -(E_T - E_{bicyclo-HMX} - E_{polymer}) \quad (1)$$

where E_T is the total energy of the PBXs, $E_{bicyclo\text{-}HMX}$ and $E_{polymer}$ are the total energies of bicyclo-HMX and fluorine polymer, respectively.

As can be seen from Fig. 3, the fluorine polymers contact closely with each crystalline surface; consequently extensive interactions exist between polymers and bicyclo-HMX. For visualization, average total energies (E_T) of the PBXs, single point energies of the base explosive ($E_{bicyclo\text{-}HMX}$) and fluorine polymers ($E_{polymer}$), and binding energies ($E_{binding}$) are presented in Table 2. It can be found that the differences not only exist in the binding energies of the PBXs with different polymers on the same crystalline surface, but also in those with the same polymer on different crystalline surfaces. With respect to different crystalline surfaces, it is obvious that bicyclo-HMX (0 1 0) surface has a stronger capability to blend with the polymers than (0 0 1) and (1 0 0) surfaces due to the larger binding energies. In other words, when fluorine polymers are put into the bicyclo-HMX crystal, they tend to concentrate on the bicyclo-HMX (0 1 0) surface due to their stronger intermolecular interactions. The van der Waals and electrostatic nonbond interactions are thought of the main origin of interactions between the fluorine polymers and bicyclo-HMX, because zero hydrogen bond energy has been included in the nonbond energies and the distances between atoms in the fluorine polymers and the crystalline surfaces are always more than 3.0 Å. Then, comparing the results of different polymer binders on the same crystalline surface, we find that there is no certain discipline in the variations of binding energies. For example, on the (0 0 1) surface the binding energy changes in the order of PCTFE > F_{2311} ≈ F_{2314} > PVDF, while those decrease in the sequences of F_{2311} > PCTFE > PVDF > F_{2314} and PVDF > F_{2311} > F_{2314} > PCTFE on the (0 1 0) and (1 0 0) surfaces, respectively.

Taking into account different mass fraction (w%) of polymers used in the PBXs, for comparison we therefore computed the average binding energy between bicyclo-HMX and a unit weight percentage of polymers according to the expression $E'_{binding} = E_{binding}/w\%$, as shown in Table 2. It is obvious that on the whole, the $E'_{binding}$ between each polymer and different crystalline surfaces changes in the order of (0 1 0) > (1 0 0) > (0 0 1), consistent with the variation of the polymers with the same chain segment on different crystalline surfaces. Furthermore, it is interesting to note that the average binding energies on each surface of bicyclo-HMX all decrease in the order of PVDF > F_{2311} > F_{2314} ≈ PCTFE. This suggests that intermolecular interactions between fluorine polymers and bicyclo-HMX decreases as PVDF > F_{2311} > F_{2314} ≈ PCTFE, and PVDF has a stronger ability to blend with the base explosive.

3.3. Mechanical property

From the elastic mechanics [35], it is known that the most general relationship between stress and strain of the material can be stated as follows by the generalized Hooke's law: $\sigma_i = C_{ij}\varepsilon_j$ (i,j = 1–6),

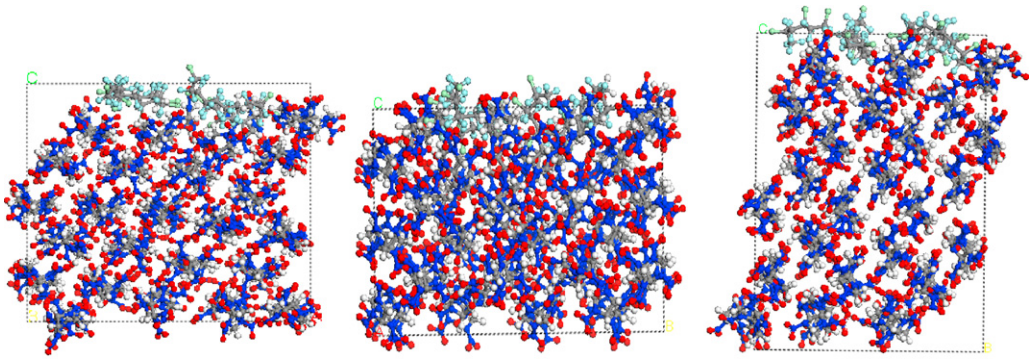

Fig. 3. Equilibrium structures of PBXs with F_{2314} on different crystalline surfaces of bicyclo-HMX. Gray, blue, red, cyan, kelly, and white spheres stand for C, N, O, F, Cl, and H atoms, respectively. (For interpretation of the references to colour in this figure legend, the reader is referred to the web version of the article.)

Table 2
Binding energies ($E_{binding}$, kcal/mol) between different fluorine polymers and crystalline surfaces of bicyclo-HMX at 298 K

PBX	Polymer	w%[a]	E_T	E_{BCHMX}	$E_{polymer}$	$E_{binding}$	$E'_{binding}$[b]
(0 0 1)	PVDF	5.87	−16988.32	−15690.59	−1144.62	153.12	26.09
	F_{2311}	8.16	−16272.54	−15663.45	−441.89	167.20	20.49
	F_{2314}	9.39	−16103.96	−15655.91	−280.96	167.09	17.79
	PCTFE	10.20	−15954.47	−15620.10	−151.06	183.30	17.97
(0 1 0)	PVDF	5.87	−16976.09	−15670.84	−1128.45	176.80	30.12
	F_{2311}	8.16	−16219.88	−15598.84	−436.75	184.28	22.58
	F_{2314}	9.39	−16005.85	−15561.73	−277.44	166.68	17.75
	PCTFE	10.20	−15888.89	−15578.84	−129.67	180.39	17.69
(1 0 0)	PVDF	5.87	−17000.21	−15693.44	−1130.32	176.45	30.06
	F_{2311}	8.16	−16291.00	−15682.36	−438.30	170.34	20.88
	F_{2314}	9.39	−16120.57	−15680.05	−280.53	159.99	17.04
	PCTFE	10.20	−15971.52	−15663.04	−149.78	158.70	15.56

[a] w% denotes the mass fraction of each fluorine polymer in the PBXs.
[b] $E'_{binding} = E_{binding}/w\%$, which means the average binding energy between a unit weight of fluorine polymer and the bicyclo-HMX crystal.

where C_{ij} are the elements of the elastic constant matrix. In principle, all mechanical properties of a material can be derived from its elastic tensors. Because of the existence of strain energy, the elastic coefficient matrix should satisfy the relationship $C_{ij} = C_{ji}$, even for an extremely anisotropic body. Therefore, there are 21 independent elastic constants in nature. The crystal symmetry can further reduce the number of independent elastic coefficients. As for the monoclinic bicyclo-HMX, there are 13 independent elastic coefficients. With regard to an isotropic solid, there are only two independent elastic constants C_{11} and C_{12}. For terseness, C_{12} and $(C_{11} - C_{12})$ are set to be equal to λ and 2μ, respectively, where λ and μ are Lamé coefficients. Accordingly, the stress–strain relationship can be described by two Lamé coefficients and the corresponding elastic constant matrix can be expressed as follows:

$$\left|C_{ij}\right| = \begin{bmatrix} \lambda+2\mu & \lambda & \lambda & 0 & 0 & 0 \\ \lambda & \lambda+2\mu & \lambda & 0 & 0 & 0 \\ \lambda & \lambda & \lambda+2\mu & 0 & 0 & 0 \\ 0 & 0 & 0 & \mu & 0 & 0 \\ 0 & 0 & 0 & 0 & \mu & 0 \\ 0 & 0 & 0 & 0 & 0 & \mu \end{bmatrix} \quad (2)$$

Therefore, all the elastic modulus, such as tensile (Young's) modulus (E), bulk modulus (K), and shear modulus (G), and Poisson's ratio (γ) can be obtained from the Lamé coefficients according to the formulas:

$$E = \frac{\mu(3\lambda+2\mu)}{\lambda+\mu},\ K = \lambda + \frac{2}{3}\mu,\ G = \mu,\ \text{and}\ \gamma = \frac{\lambda}{2(\lambda+\mu)}.$$

On the basis of NVT-MD simulation trajectories and the elastic-static method, the second order elastic tensors and various moduli of bicyclo-HMX have been studied at ambient condition. Here, it should be pointed that the elastic analysis methods implemented in the MS all assume the material to be isotropic as they calculate the Poisson's ratio and various moduli, so we could not report directly the mechanical properties along the various crystallographic directions. That is, only the effective isotropic Poisson's ratio and various moduli are obtained. And there are no experimental determinations or theoretical predictions available on the elastic constants or stress–strain relationship of bicyclo-HMX or its PBXs, we hence cannot make any comparison but only compare the results of the PBXs with those of the pure crystal to investigate the polymer effect.

From the elastic coefficient matrix of pure crystal bicyclo-HMX in Table 3 it can be found that all diagonal elements C_{ii} and the off-diagonal elements C_{12}, C_{13}, C_{23} are larger than other elements, indicating considerable anisotropy of the crystal. This characteristic can be further proved by the differences in the elastic coefficients of the PBXs with the same fluorine polymer on three crystal surfaces. Compared with the pure bicyclo-HMX, the smaller diagonal element C_{11} increases for all PBXs, while other diagonal elements C_{ii} all decrease except C_{33} of the PBXs with fluorine polymer on bicyclo-HMX (0 1 0) surface and C_{44} on (1 0 0) surface. Moreover, the off-diagonal elements C_{15}, C_{23}, C_{25}, C_{35}, and C_{46} decrease to some extent while C_{12} and C_{13} increase slightly. This evolution tendency of elastic coefficients shows that adding small amounts of fluorine polymers can reduce the anisotropy of the system.

Cauchy pressure $(C_{12} - C_{44})$ can be used as a criterion to evaluate the ductibility or brittleness of a material. As a rule, the value of $(C_{12} - C_{44})$ for a ductile material is positive; on the contrary, that is negative for a brittle material. Meanwhile, the more positive the $(C_{12} - C_{44})$ value is the more ductile the material is. According to this, the data in the last column of Table 3 indicate that the pure bicyclo-HMX and the obtained PBXs are all ductile due to their positive $(C_{12} - C_{44})$. But, the Cauchy pressures of the PBXs are all larger than that of the pure crystal, except the PBX with PVDF on the bicyclo-HMX (0 1 0) surface. This indicates that the ductibility of bicyclo-HMX is greatly improved by adding small quantities of fluorine polymers. Comparing the values of $(C_{12} - C_{44})$ for each polymer on different crystalline surfaces of bicyclo-HMX, we find that the ductibility of PBXs depends on different surfaces, and it changes in the following order: (1 0 0) > (0 0 1) > (0 1 0). It can also be found that for each crystalline surface of bicyclo-HMX, PCTFE always improves the ductibility of PBXs; and when it was put on the bicyclo-HMX (1 0 0) surface, the obtained PBX has the best ductibility with the Cauchy pressure $(C_{12} - C_{44})$ of 4.1 GPa.

Table 4 shows the effective isotropic mechanical properties of the pure crystal bicyclo-HMX and PBXs at 298 K, including tensile modulus E, bulk modulus K, shear modulus G, and Poisson's ratio γ. All the moduli can be used to measure the extent of rigidity or stiffness of a material, i.e. an indication of the capability of a material to resist the changes of shape or volume caused by external stress. Meanwhile, the resistance to plastic deformation is proportional to the shear modulus G and the fracture strength is proportional to the bulk modulus K [36]. The larger the moduli, the stiffer the material, and the smaller the deformation of the material. According to these, it can be deduced that the rigidity and brittleness of the bicyclo-HMX-based PBXs decrease while their elasticity and plasticity strengthen, because in comparison with those of the pure crystal the moduli of all PBXs decrease with several exceptions. These variations also suggest that the mixed explosives will deform more easily than the monoexplosive when they are subjected to an external force. The content of polymers in the simulated PBXs is about 5–10%, which is nearly equivalent to the ratio of polymer in the practical PBXs. Therefore, the mechanical properties of the explosive can be effectively improved by blending

Table 3
Elastic constants (GPa) of pure crystal bicyclo-HMX and bicyclo-HMX-based PBXs with different polymers binding on different crystalline surfaces at 298 K

PBX	Polymer	C_{11}	C_{22}	C_{33}	C_{44}	C_{55}	C_{66}	C_{12}	C_{13}	C_{15}	C_{23}	C_{25}	C_{35}	C_{46}	$C_{12}-C_{44}$
BCHMX		6.6	16.4	9.2	3.2	5.5	4.3	5.0	3.2	0.0	7.9	2.0	0.5	0.6	1.8
(0 0 1)	PVDF	10.4	12.5	8.8	3.2	3.4	3.4	5.4	5.2	−0.2	6.3	0.5	0.1	0.4	2.2
	F_{2311}	10.4	12.1	9.0	2.5	2.6	2.8	4.7	5.0	−0.3	6.2	0.7	0.2	0.0	2.2
	F_{2314}	11.6	12.0	10.5	2.5	3.0	2.8	4.9	5.4	0.2	6.3	0.6	0.1	0.7	2.4
	PCTFE	11.3	12.3	8.9	3.0	2.7	3.4	5.2	5.5	−0.5	6.1	0.1	−0.1	0.1	2.2
(0 1 0)	PVDF	9.3	10.5	10.7	3.5	3.7	3.6	5.0	5.6	0.2	5.6	0.3	0.2	0.4	1.5
	F_{2311}	8.5	10.1	10.3	2.8	3.4	3.0	4.9	5.4	0.1	4.9	−0.1	0.3	−0.4	2.1
	F_{2314}	8.8	7.2	10.3	2.8	2.9	3.4	5.2	5.3	0.1	4.9	−0.1	0.1	0.2	2.4
	PCTFE	8.9	9.0	10.2	3.0	3.3	3.3	5.2	6.4	−0.2	5.5	−0.2	−0.2	−0.2	2.2
(1 0 0)	PVDF	13.0	9.4	9.4	3.1	2.8	3.0	6.2	5.3	−0.2	4.3	0.0	0.2	0.0	3.1
	F_{2311}	12.8	8.4	9.0	3.1	2.1	2.4	6.1	4.9	−0.1	3.7	0.5	0.1	0.0	3.0
	F_{2314}	12.5	9.8	9.3	3.5	2.5	2.7	6.5	4.7	0.3	4.6	0.4	0.3	0.0	3.0
	PCTFE	12.7	8.8	9.6	3.5	2.3	2.8	7.6	4.1	0.1	4.1	0.3	0.0	0.2	4.1

the polymers as a binder in a small amount. This is consistent with previous studies on the HMX-, TATB-, TNAD-, and CL20-based PBXs. The differences among the moduli of different PBXs with fluorine polymers on each crystalline surface are not very evident because the anisotropic behaviour of PBXs has been improved. However, the effect of polymers on improving the mechanical properties of different crystal surfaces is somewhat different and changes in the order of (0 1 0) > (0 0 1) ≈ (1 0 0) on the whole. And F_{2314} is regarded as the best binder for improving the mechanical properties of PBX on the bicyclo-HMX (0 1 0) surface. Furthermore, the Poisson's ratio correlates various isotropic moduli through the formula $E = 3K(1-2\gamma) = 2G(1+\gamma)$, which can be used to evaluate the plasticity of the material. Comparison of the Poisson's ratios shows that pure bicyclo-HMX and all PBXs possess superior plastic properties since they have larger Poisson's ratio (>0.3). In general, the Poisson's ratio of a plastic is 0.2–0.4.

Furthermore, the ratio of bulk modulus to shear modulus (K/G) can be used as an indication of the extent of the plastic range for a material. Usually, a larger value of K/G is associated with a better malleability of the material [36]. According to this, it can be found from the K/G values in Table 4 that the malleability of PBXs with fluorine polymers on different crystalline surfaces decreases as (0 1 0) > (0 0 1) ≈ (1 0 0), and the PBX with PCTFE on bicyclo-HMX (0 1 0) surface is expected to possess the best malleability ($K/G = 3.77$). Compared with the pure crystal, the malleability only increases for the PBXs with polymer binders on the bicyclo-HMX (0 1 0) crystalline surface, while those with polymer binders on the (0 0 1) and (1 0 0) surfaces change a little and some even decrease. Considered two aspects comprehensively, mechanical property and adhesive property (binding energy), it is found that the PBXs with fluorine polymers on bicyclo-HMX (0 1 0) crystalline surface are superior to other systems. This may be instructive for the formulation design of bicyclo-HMX-based PBXs.

3.4. Detonation performance

Density (ρ), detonation heat (Q), detonation velocity (D), and detonation pressure (P) are important parameters to evaluate the explosive performances of energetic materials. Up to now, many theoretical and empirical methods have been suggested to evaluate these detonation properties, such as the Urizar formula [16], Kamlet–Jacobs equations [37], and ω–Γ method [38]. The ω–Γ method suggested by Wu is selected for our calculations because it is more suitable for both the pure and mixed explosives. In this method, detonation heat Q (J/g), detonation velocity D (m/s), and detonation pressure P (GPa) are calculated according to the following definitions:

$$Q = \frac{\Delta H_f - \sum n_i \Delta H_i}{M} \tag{3}$$

$$D = 33.05Q^{1/2} + 243.2\omega\rho \tag{4}$$

$$P = \frac{\rho D^2 \times 10^{-6}}{\Gamma + 1} \tag{5}$$

where n_i and M respectively denote the amount of the ith detonation product (mol) and the molecular weight of the explosive (g/mol); ΔH_i and ΔH_f represent the heat of formation (J/mol) of the ith detonation product and the explosive, respectively; ρ, ω, and Γ are the loaded density of explosive (g/cm^3), the factor of potential energy, and the adiabatic exponent, respectively. As for

Table 4
Effective isotropic mechanical properties of pure crystal bicyclo-HMX and bicyclo-HMX-based PBXs at 298 K

PBX	Polymer	Tensile modulus, E (GPa)	Bulk modulus, K (GPa)	Shear modulus, G (GPa)	Poisson's ratio, (γ)	K/G
BCHMX		7.15	7.15	2.68	0.33	2.67
(0 0 1)	PVDF	6.67	7.27	2.48	0.35	2.93
	F_{2311}	6.94	7.04	2.60	0.34	2.71
	F_{2314}	7.69	7.49	2.89	0.33	2.59
	PCTFE	6.98	7.36	2.60	0.34	2.83
(0 1 0)	PVDF	6.49	6.99	2.41	0.35	2.90
	F_{2311}	6.18	6.60	2.30	0.34	2.87
	F_{2314}	4.96	6.34	1.81	0.37	3.50
	PCTFE	5.07	6.93	1.84	0.38	3.77
(1 0 0)	PVDF	7.07	7.06	2.65	0.33	2.66
	F_{2311}	6.87	6.62	2.59	0.33	2.56
	F_{2314}	7.01	7.03	2.63	0.33	2.67
	PCTFE	7.49	6.79	2.85	0.32	2.38

Table 5
Predicted detonation performances of pure crystal bicyclo-HMX and PBXs with different fluorine polymers on the bicyclo-HMX (0 1 0) surface

Parameter	BCHMX	BCHMX/PVDF	BCHMX/F_{2311}	BCHMX/F_{2314}	BCHMX/PCTFE
Q (J/g)	6518	6258	6157	6102	6066
ρ (g/cm^3)	1.861	1.849(1.852)[a]	1.859(1.864)[a]	1.875(1.876)[a]	1.881(1.885)[a]
D (m/s)	8792	8555(8564)[b]	8506(8522)[b]	8514(8518)[b]	8507(8520)[b]
P (GPa)	35.96	33.83(33.96)[b]	33.63(33.85)[b]	33.98(34.02)[b]	34.03(34.21)[b]

[a] Values in the parentheses are the predicted maximum densities of PBXs according to their compositions.
[b] Data in the parentheses are the predicted detonation performances based on the maximum densities of the PBXs.

the blended explosives, the Q, ρ, ω, and Γ are evaluated by summing up the Q_i, ρ_i, ω_i, and Γ_i of each component, respectively, according to their mass percent. Since the PBX containing the fluorine element is complex, the Γ is difficult to obtain. Therefore, according to the C–J theory [39], the Eq. (5) can be simplified as follows to evaluate the detonation pressure of the PBX:

$$P = \frac{1}{4}\rho D^2 \times 10^{-6} \quad (6)$$

In the light of the conclusion drawn from the above sections, we chose the bicyclo-HMX (0 1 0) surface as a model to calculate the PBXs' detonation performances. The predicted results are listed in Table 5 and compared with those of the pure crystal. Several characteristics can be observed. First, detonation properties Q, D, and P of all the PBXs are smaller than those of the pure explosive except that the densities of bicyclo-HMX/F_{2314} and bicyclo-HMX/PCTFE are slightly larger than that of the pure crystal. This is attributed to the fact that the fluorine polymers F_{2314} and PCTFE have larger ρ than bicyclo-HMX. However, all the polymer binders have smaller Q than the pure crystal, so the PBXs possess lower Q, D, and P than pure bicyclo-HMX. But, compared with the famous explosive TNT (2,4,6-trinitrotoluene) (ρ = 1.64 g/cm^3, D = 6.95 km/s, P = 19.0 GPa) [17], it is obvious that all the PBXs designed in this paper have better detonation performances than TNT. That is to say, these PBXs can still be considered as potential candidates of energetic materials with good performances. Therefore, if these stable PBXs can be prepared, they will have higher exploitable values and be worth investigating further.

Also noteworthy is that detonation velocity and pressure of the simulated PBXs are all smaller than those predicted on the basis of theoretical maximum densities although the discrepancies are trivial. This may be attributed to the voids caused by intermolecular interactions in the simulated boxes, while such interactions are absent in the theoretical predictions according to their compositions. In addition, it is found that there is no evident discrepancy among the detonation properties of these PBXs. This may be partially originated from the calculation method in which the same values of Q (2090.0 J/g) and ω (8.0) are used for different fluorine polymers, respectively, but in fact they are different from each other. On the whole, one can conclude that these four kinds of fluorine polymers with the same chain segments have similar effects on the detonation properties of the bicyclo-HMX-based PBXs.

4. Conclusions

In this study, we have performed MD simulations to study the binding energies, mechanical properties, and detonation performances of the bicyclo-HMX-based PBXs. The effects of different fluorine polymers on different crystalline surfaces are investigated. The major findings can be summarized as follows:

(1) The binding energies between different crystalline surfaces and polymers with the same chain segment or mass fraction both decrease in the order of (0 1 0) > (1 0 0) > (0 0 1) on the whole. On each crystalline surface, binding properties for the polymers with the same chain segments are not consistent with each other, while those for the polymers with the same content all decrease in the order of PVDF > F_{2311} > F_{2314} ≈ PCTFE.
(2) The mechanical properties of the pure bicyclo-HMX can be effectively improved by adding small amounts of fluorine polymers. On three different crystalline surfaces, the effect of fluorine polymers on improving the mechanical properties is approximately (0 1 0) > (0 0 1) ≈ (1 0 0), whereas the improvement in the ductibility ($C_{12} - C_{44}$) made by the fluorine polymers changes in the sequence of (1 0 0) > (0 0 1) > (0 1 0).
(3) The predicted detonation performances show that all the bicyclo-HMX-based PBXs are superior to the explosive TNT and can be used as good energetic materials, although they decrease slightly in comparison with the pure crystal. Due to intermolecular interactions existing in the bulk, detonation performances of the simulated PBXs are smaller than those evaluated according to their components. Four fluorine polymers with the same chain segment have similar effect on the PBXs' detonation performances.

In a word, the MD simulations on the bicyclo-HMX-based PBXs provide us much information about their adhesive properties, mechanical properties, and detonation performances, which may be helpful for screening proper polymer binders and crystal surfaces to design novel PBXs with different performances according to the practical requirements.

Acknowledgements

We are very grateful for the financial support from the National Natural Science Foundation of China (Grant Nos. 10576030 and 10576016) and the National "973" Project.

Appendix A. Supplementary data

Supplementary data associated with this article can be found, in the online version, at doi:10.1016/j.jhazmat.2008.08.030.

References

[1] C.L. Coon, Research on the Synthesis of Heterocyclic Explosives, in: Proceedings of the UCRL-95288 DE87001360 American Defense Preparedness Symposium, Lawrence Livermore National Lab CA, USA, 20 August, 1986.
[2] T.B. Brill, Y. Oyumi, Thermal decomposition of energetic materials. 9. A relationship of molecular structure and vibrations to decomposition: polynitro-3,3,7,7-tetrakis(trifluoromethyl)-2,4,6,8-tetraazabicyclo[3.3.0]octanes, J. Phys. Chem. 90 (1986) 2679–2682.
[3] W.M. Koppes, M. Chaykovsky, H.G. Adolph, R. Gilardi, C. George, Synthesis and structure of some peri-substituted 2,4,6,8-tetraazabicyclo[3.3.0]octanes, J. Org. Chem. 52 (1987) 1113–1119.
[4] A.T. Nielsen, R.A. Nissan, A.P. Chafin, Polyazapolycyclics by condensation of aldehydes with amines. 3. Formation of 2,4,6,8-tetrabenzyl-2,4,6,8-tetraazabicyclo[3.3.0]octanes from formaldehyde, glyoxal, and benzylamines, J. Org. Chem. 57 (1992) 6756–6759.
[5] G.T. Afanas'ev, T.S. Pivina, D.V. Sukhachev, Comparative characteristics of some experimental and computational methods of estimating impact sensitivity parameters of explosives, Propell. Explos. Pyrotech. 18 (1993) 309–316.

[6] P.F. Pagoria, A.R. Mitchell, R.D. Schmidt, C.L. Coon, E.S. Jessop, New nitration and nitrolysis procedures in the synthesis of energetic materials, ACS Symp. Ser. 623 (1996) 151–164.
[7] G. Eck, M. Piteau, Preparation of 2,4,6,8-tetranitro-2,4,6,8-tetraazabicyclo [3.3.0]octane. Brit. UK Patent Appl. GB 2303849 A1, (5 March 1997), 9 pp.
[8] D. Skare, Tendencies in development of new explosives. Heterocyclic, benzenoid-aromatic and alicyclic compounds, Kem. Ind. 48 (1999) 97–102.
[9] C. Cai, C.X. Lu, Synthesis of 2,4,6,8-tetrasubstituted-2,4,6,8-tetraazabicyclo[3,3,0]octanes, Nanjing Ligong Daxue Xuebao 23 (1999) 253–256.
[10] R. Gilardi, J.L. Flippen-Anderson, R. Evans, *cis*-2,4,6,8-Tetranitro-1H,5H-2,4,6,8-tetraazabicyclo[3.3.0]octane, the energetic compound 'bicyclo-HMX', Acta Crystallogr. E 58 (2002) 972–974.
[11] L. Qiu, H.M. Xiao, X.H. Ju, X.D. Gong, Theoretical study on the pyrolysis mechanisms of tetranitrotetraazabicyclooctane in gas phase, Energy Mater. 13 (2005) 74–78.
[12] L. Qiu, H.M. Xiao, X.H. Ju, X.D. Gong, Theoretical study on the structures and properties of bicyclo-HMX, Acta Chim. Sin. 63 (2005) 377–384.
[13] L. Qiu, X.H. Ju, H.M. Xiao, Density functional theory study of solvent effects on the structure and vibrational frequencies of tetranitrotetraazabicyclooctane "bicyclo-HMX", J. Chin. Chem. Soc. 52 (2005) 405–413.
[14] L. Qiu, W.H. Zhu, J.J. Xiao, H.M. Xiao, Theoretical studies of solid bicyclo-HMX: effects of hydrostatic pressure and temperature, J. Phys. Chem. B 112 (2008) 3882–3893.
[15] G.X. Sun, Polymer Blended Explosives, Defense Industry Press, Beijing, 1984.
[16] B.M. Dobratz, P.C. Crawford, LLNL Explosives Handbook—Properties of Chemical Explosives and Explosive Simulants; UCRL-52997, Lawrence Livermore National Laboratory, Livermore, CA, 1985.
[17] H.S. Dong, F.F. Zhou, Performance of High Energetic Explosive and Related Compounds, Science Press, Beijing, 1989.
[18] Y.B. Sun, J.M. Hui, X.M. Cao, Military Use Blended Explosives, Weapon Industry Press, Beijing, 1995.
[19] A.S. Tompa Dr., R.F. Boswell, Thermal stability of a plastic bonded explosive, Thermochim. Acta 357–358 (2000) 169–175.
[20] M.S. Campbell, D. Garcia, D. Idar, Effects of temperature and pressure on the glass transitions of plastic bonded explosives, Thermochim. Acta 357–358 (2000) 89–95.
[21] J.S. Lee, C.K. Hsu, Thermal properties and shelf life of HMX–HTPB-based plastic-bonded explosives, Thermochim. Acta 392–393 (2002) 153–156.
[22] B. Banerjee, D.O. Adams, Micromechanics-based determination of effective elastic properties of polymer bonded explosives, Phys. B: Condens. Matter 338 (2003) 8–15.
[23] C.M. Tarver, T.D. Tran, Thermal decomposition models for HMX-based plastic bonded explosives, Combust. Flame 137 (2004) 50–62.
[24] D.S. Thomas, M. Ralph, B. Dmitry, D.S. Grant, A molecular dynamics simulation study of elastic properties of HMX, J. Chem. Phys. 119 (2003) 7417–7426.
[25] R.H. Gee, S. Roszak, K. Balasubramanian, L.E. Fried, Ab initio based force field and molecular dynamics simulations of crystalline TATB, J. Chem. Phys. 120 (2004) 7059–7066.
[26] (a) D.C. Sorescu, D.L. Thompson, Classical and quantum mechanical studies of crystalline ammonium dinitramide, J. Phys. Chem. B 103 (1999) 6774–6782;
(b) D.C. Sorescu, J.A. Boatz, D.L. Thompson, Classical and quantum-mechanical studies of crystalline FOX-7 (1,1-diamino-2,2-dinitroethylene), J. Phys. Chem. A 105 (2001) 5010–5021;
(c) D.C. Sorescu, D.L. Thompson, Classical and quantum mechanical studies of crystalline ammonium nitrate, J. Phys. Chem. A 105 (2001) 720–733;
(d) G.F. Velardez, S. Alavi, D.L. Thompsona, Molecular dynamics studies of melting and liquid properties of ammonium dinitramide, J. Chem. Phys. 119 (2003) 6698–6708.
[27] (a) Y.C. Huang, Y.J. Hu, J.J. Xiao, K.L. Yin, H.M. Xiao, Molecular dynamics simulation of binding energies of TATB-based PBX, Acta Phys. Chim. Sin. 21 (2005) 425–429;
(b) J.J. Xiao, G.Y. Fang, G.F. Ji, H.M. Xiao, Simulation investigation in the binding energy and mechanical properties of HMX-based polymer-bonded explosives, Chin. Sci. Bull. 50 (2005) 21–26;
(c) L. Qiu, W.H. Zhu, J.J. Xiao, W. Zhu, H.M. Xiao, H. Huang, J.S. Li, Molecular dynamics simulations of TNAD (*trans*-1,4,5,8-tetranitro-1,4,5,8-tetraazadecalin)-based PBXs, J. Phys. Chem. B 111 (2007) 1559–1566;
(d) X.J. Xu, H.M. Xiao, J.J. Xiao, W. Zhu, H. Huang, J.S. Li, Molecular dynamics simulations for pure ε-CL-20 and ε-CL-20-based PBXs, J. Phys. Chem. B 110 (2006) 7203–7207.
[28] Materials Studio 3.0.1, Accelrys Inc. San Diego, CA, 2004.
[29] H. Sun, Compass: an ab initio force-field optimized for condense-phase applications-overview with details on alkanes and benzene compounds, J. Phys. Chem. B 102 (1998) 7338–7364.
[30] H.C. Andersen, Molecular dynamics simulations at constant pressure and/or temperature, J. Chem. Phys. 72 (1980) 2384–2393.
[31] M.P. Allen, D.J. Tildesley, Computer Simulation of Liquids, Oxford University Press, New York, 1989.
[32] H. Sun, D. Rigby, Polysiloxanes: ab initio force and structural, conformational and thermophysical properties, Spectrochim. Acta A 153 (1997) 1301–1323.
[33] D. Rigby, H. Sun, B.E. Eichinger, Computer simulations of poly(ethylene oxide): force field, pvt diagram and cyclization behaviour, Polym. Int. 44 (1997) 311–330.
[34] T. Spyriouni, C. Vergelati, A molecular modeling study of binany blend compatibility of polyamide 6 and poly(vinyl acetate) with different degrees of hydrolysis:an atomistic and mesoscopic approach, Macromolecules 34 (2001) 5306–5316.
[35] J.H. Weiner, Statistical Mechanics of Elasticity, John Wiley, New York, 1983.
[36] S.F. Pugh, Relation between the elastic moduli and the plastic properties of polycrystalline pure metals, Philos. Mag. 45 (1954) 823–843.
[37] M.J. Kamlet, S.J. Jacobs, Chemistry of detonations. I. Simple method for calculating detonation properties of C–H–N–O explosives, J. Chem. Phys. 48 (1968) 23–35.
[38] X. Wu, Simple method for calculating detonation parameters of explosives, J. Energy Mater. 3 (1985) 263–277.
[39] X.C. Meng, J.X. Zhang, Introduction of Detonation Theory, Beijing Institute of Technology Press, Beijing, 1988.